*BME Horizon* Vol 1 Issue 1 2023
DOI: 10.37155/2972–449X–0101–3

ORIGINAL RESEARCH ARTICLE

Open Access

# Stretchable and Self-Adhesive PEDOT:PSS/MXene Dry Electrode with Low Contact Impedance for ECG Monitoring

**Xianglin Gao, Tong Su, Yilin Bao, Jipei Lu and Lei Zhang***

Department of Biomedical Engineering & Instrument Science, Key Laboratory for Biomedical Engineering of Ministry of Education, Zhejiang University, Hangzhou, 310027, China;

***Correspondence to:** Lei Zhang, Department of Biomedical Engineering & Instrument Science, Key Laboratory for Biomedical Engineering of Ministry of Education, Zhejiang University, Hangzhou, 310027, China; Email: leimxi@zju.edu.cn

**Received:** April 4, 2023; **Accepted:** June 10, 2023; **Published Online:** June 20, 2023

**How to cite:** Xianglin Gao, Tong Su, Yilin Bao, Jipei Lu and Lei Zhang. Stretchable and Self-Adhesive PEDOT:PSS/MXene Dry Electrode with Low Contact Impedance for ECG Monitoring. *BME Horizon*, 2023; 1(1):57. DOI: 10.37155/2972-449X-0101-3

**Abstract:** Wearable dry electrodes are necessary for the long-term recording of human biopotential signals. However, current dry electrode may not fit the skin thoroughly, particularly when there is movement and sweat secretion which can lead to high interface impedance and poor signal quality. In this work, a stretchable dry electrode with low contact impedance and good self-adhesiveness has been prepared by solution processed conductive PEDOT:PSS, MXene, waterborne polyurethane (WPU) and fructose. The resultant dry electrode with excellent skin compliance shows much lower skin-contact impedance than the standard silver/silver chloride (Ag/AgCl) gel electrodes, and enables acquisition of high-quality electrocardiogram (ECG) signal under dry and wet skin conditions. The dry electrode shows promise in supporting application of ECG monitoring in daily scenarios.

**Keywords:** PEDOT:PSS; MXene; Dry electrode; ECG

## 1. Introduction

Electrocardiogram (ECG) plays an essential role in diagnosing and treating heart-related diseases. ECG signals can be transduced by the epidermal electrode. Efficient wearable electrodes are essential for accurately recording these biopotential signals, especially in continuous monitoring of subclinical heart disease and cardiac rehabilitation[1]. Ag/AgCl gel electrodes are dominant in clinical practice, but they are prone to signal attenuation in long-term continuous monitoring due to the evaporation of liquid in the gel electrolyte, which

can result in skin irritation[2]. Therefore, efforts have been devoted to the development of skin-friendly dry electrodes for wearable ECG measurements. Dry electrodes in the literature can be mainly divided into contact dry electrodes and non-contact dry electrodes (capacitance-based)[3]. The contact dry electrodes that attach closely with skin have more stable recording interfaces and show much higher signal to noise ratio (SNR)[4]. To construct a dry electrode compliant with skin, flexible contact dry electrodes are commonly prepared by thin metal films[5,6], conductive polymer composites[7], and intrinsically conductive polymers[2]. Although the metallic films can be highly conductive[8], they are not stretchy and adhesive. Additionally, the metallic dry electrodes usually suffer from remarkable motion artifacts during body movement and high contact impedance on the skin[9,10]. By contrast, soft conductive polymer composites and intrinsically conductive polymers have good adaptation to rough and even deformed skin, and are used to prevalently prepare stretchable skin electrode[11]. Conductive polymer composites consist of elastomers and conductive nanofillers, such as carbon and metal nanotubes[12], nanowires[13]. Yao *et al*. combined Ecoflex with Ag nanowires in a 3D template to form a stretchable and adhesive electrode, but the contact impedance between skin and electrode is unsatisfactorily high[14]. To balance the mechanical properties and conductivity, the volume ratio of conductive nanofillers is low in the elastic matrix[15], resulting in a small effective contact area between conductive nanofillers and human skin and resulting in high contact impedance[16]. Therefore, the contact impedance on the skin is several orders of magnitude higher than that of Ag/AgCl gel electrodes, leading to a unsatisfactory SNR. There is also concern about the toxicity of the nanofillers[17-19].

Intrinsically conductive polymers have the advantages of good flexibility and effective contact interface with skin, as well as high conductivity and good biocompatibility[20]. As one of the typical representative, Poly (3,4-ethylenedioxythiophene): poly(styrenesulfonate) (PEDOT:PSS) has received particular attention, due to its high conductivity and outstanding biocompatibility[21]. For example, Li *et al*. reported a flexible paper-based skin electrode for the detection of ECG signal , in which a highly conductive PEDOT:PSS hydrogel was coated on the paper fibers[22]. Roberts *et al*. constructed an PEDOT:PSS array on the polyimide by inkjet printing technology, showing comparable ECG recording performance to the commercial Ag/AgCl electrode[23]. Although there flexible electrodes can record ECG signal at rest state, they are not stretchable and are not capable of attaching tightly on the deformed skin during body movement. PEDOT:PSS with conjugated PEDOT domain is non-stretchable intrinsically[24,25], which affects the electrode performance on the deformed skin. To improve the stretchability of PEDOT:PSS, some additives such as surfactants and hydrophilic polymer are used to dope PEDOT:PSS[21]. But these non-conductive components decrease the conductivity of PEDOT:PSS composites. Bao *et al*. created highly stretchable and conductive PEDOT films by incorporating ionic additives, achieving a high conductivity over 4100 S/cm under 100% strain[26]. Liu *et al*. reported an ultra-thin dry epidermal electrode that is able to conformably adhere to skin by incorporating PEDOT:PSS with graphene and ionic liquid. These conformable thin film electrodes comply well with skin and record high quality ECG signal[27]. But the concerns about the skin irritation of ionic additives still limit their applications in the epidermal dry electrodes.

$Ti_3C_2T_x$ is a typical representative of 2D layered MXenes, which has ultra-high conductivity up to ~10000 S $cm^{-1}$ and high capacitance up to ~1500 F $cm^{-3}$[28]. Highly conductive MXene nanosheets can be incorporated with other conductive materials, such as silver nanowires, carbon nanotube, or graphene to enhance the conductivity of their composites with lower loading of nanofillers[29,30]. This synergistic effect can help to avoid compromising high conductivity and high mechanical stretchability[31]. The hydrophilic MXene nanosheets dispersion is expected to blend with PEDOT:PSS to enhance its conductivity[32,33]. However, blending MXene uniformly with PEDOT:PSS and fabricating an epidermal dry electrode with low contact impedance and good stretchability remain challenges.

We fabricated a stretchable and self-adhesive dry electrode with low skin impedance by solution processing biocompatible blends of PEDOT:PSS, MXene, waterborne polyurethane (WPU), and fructose. PEDOT:PSS is uniformly blended with MXene with

assistance of fructose. The resulting dry electrode (PMWF) shows good compliance and adhesiveness with skin and high conductivity, which leads to much lower impedance than the standard Ag/AgCl gel electrode. Therefore, the prepared dry electrode displays a high SNR level in static detection of ECG signals.

## 2. Materials and Method

### 2.1 Materials

PEDOT:PSS aqueous solution (Clevios PH 1000) was purchased from Heraeus Co., Ltd (Leverkusen, Germany). The concentration of PEDOT: PSS in the solution is 1.3%, and the weight ratio of PSS to PEDOT is about 2.5:1. WPU (WPU-517, 30 wt%) was provided by Anhui Chunxiao Chemical Industry (Anhui, China). Fructose and ethylene glycol were obtained from Macklin Inc. (Shanghai, China). $Ti_3AlC_2$ powder (200 mesh) was purchased from Yiyi Technology Co., Ltd (Shenzhen, China). Lithium fluoride (LiF) was purchased from Aladdin Biochemical Technology Co., Ltd. (Shanghai, China). Concentrated hydrochloric acid (HCl, 37 wt%) was obtained from Sinopharm Chemical Reagent Co., LTD (Shanghai, China). All chemicals are used directly without further treatment.

### 2.2 Preparation of MXene Nanosheets

The concentrated hydrochloric acid was diluted to 9 M using deionized water in a Teflon beaker, 0.5 g of LiF was slowly added into the 9 M of HCl solution and was stirred on a magnetic stirrer for 30 min at 400 rpm[33]. Subsequently, 0.5 g of $Ti_3AlC_2$ powder was added slowly into the LiF/HCl solution in batches, and the mixture was continuously stirred for 24 h at 40 °C. The precipitate was centrifuged at 3500 rpm for 10 min and washed with deionized water for several cycles until the pH of the supernatant was above 5, and the ink-like precipitate was a single layer MXene nanosheets. Before using, the precipitate was dispersed in deionized water and sonicated for 30 min to achieve a uniform MXene dispersive solution.

### 2.3 Fabrication of PMWF Dry Electrode

PEDOT:PSS was blended with 5 % of ethylene glycol (v/v) and stirred for 30 min at room temperature. Then diluted WPU solution (10%), fructose aqueous solution (10%) and MXene solution (11.5%) were added successively in the above PEDOT:PSS solution and stirred for 30 min at room temperature. Then the mixture solution was dropped into a Teflon Petri dish and dried at 70 °C for over 1 hour to get the PMWF film. The resulting PMWF film was cut into a circle shape with a diameter of 3 cm and attached with a button electrode on the center, achieving the final wearable PMWF dry electrode for ECG signal detection.

### 2.4 Characterization

The microstructures of the MXene nanosheets and dry electrode were observed by scanning electron microscope (SEM, Hitachi SU-70) and transmission electron microscope (TEM, HT-7700). The impedance measurement of the PMWF dry electrode was performed by the CHI600E electrochemical workstation of Shanghai Chenhua Instrument Co., LTD (Shanghai, China) in the frequency range of 1 to 10 kHz. The commercial Ag/AgCl gel electrode served as a reference electrode. The film conductivity was measured by the four-wire method using a Keysight B2901A digital source meter. The tensile properties of the blend film were measured by the American Mark-10 company ESM303 universal material testing machine, the sensor range is 25 N, and the tensile speed is 2.0 mm/min. ECG signals were acquired by placing two PMWF film electrodes on the wrist and a reference electrode on the backhand. The electrodes were connected to a signal recording device processed with a bandpass filter of 0.5-150 Hz. The signal recording setup has two parts, including a microcontroller (Arduino UNO microcontroller) and a detector (SpikerBox Pro). The ECG was captured by Spikershield. Matlab was used to control the acquisition signal and do subsequent processing.

## 3. Result and Discussion

The fabrication process of the dry electrodes is shown in **Figure 1**. To enhance the conductivity of the dry electrode, highly conductive MXene nanosheets are incorporated with flexible conductive polymer PEDOT:PSS. The MXene nanosheets are prepared by the typical etching process of $Ti_3AlC_2$ powder with a mixing LiF/HCl solution. Although PEDOT:PSS and MXene nanosheets have good electrical conductivity, the stretchability of both two materials is limited.[34] Elastic waterborne polyurethane (WPU) blends well with PEDOT:PSS and MXene to get a stretchable conductive film. Fructose is a biocompatible

polyhydroxy compound and introduces in the composite to improve the interfacial adhesion of the dry electrode with the skin (**Figure 1a**).

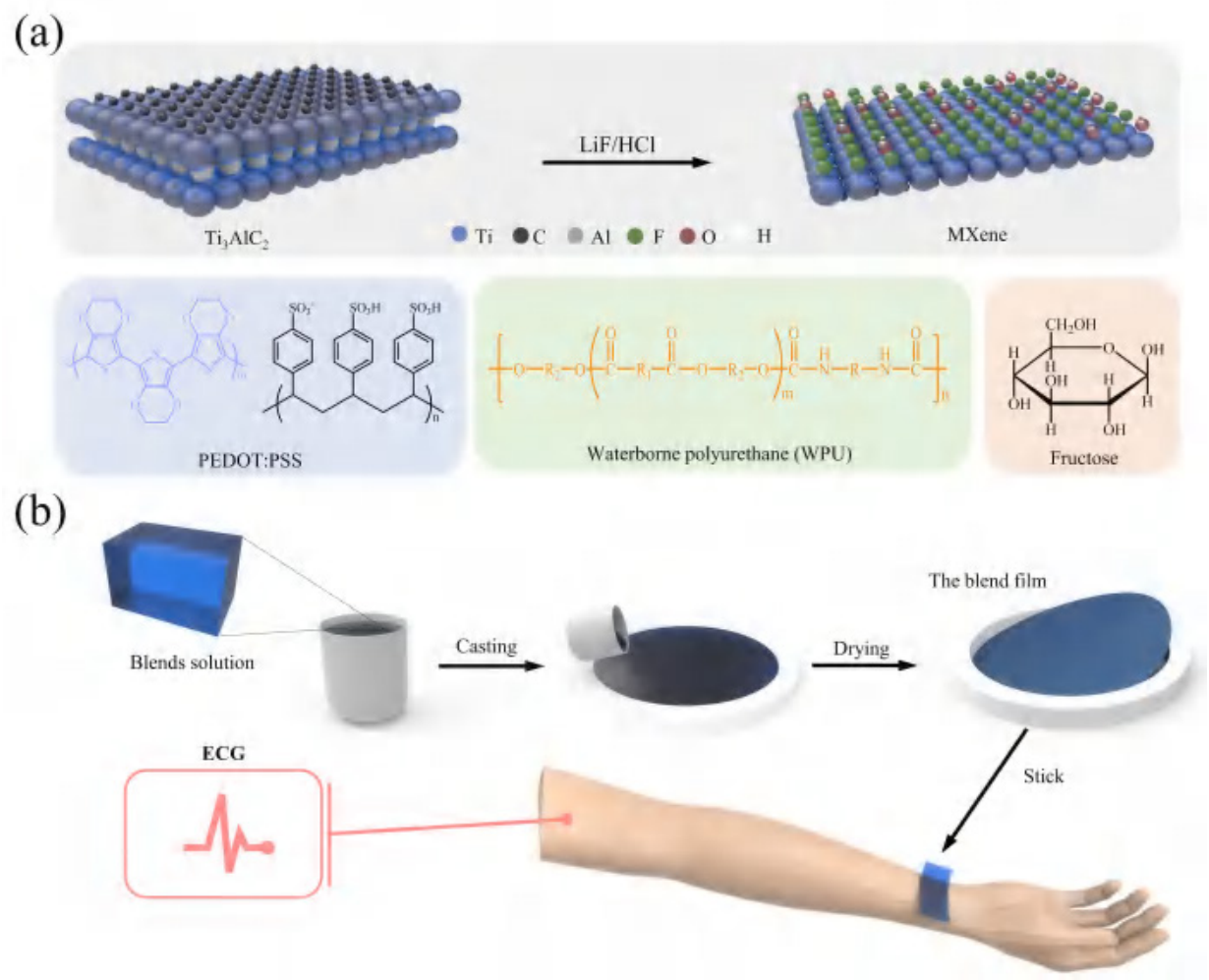


**Figure 1.** Schematic diagram of the preparation of the PMWF dry electrode. **(a)** PMWF dry electrode is composed of conductive MXene nanosheet and PEDOT:PSS, elastic waterborne polyurethane, and fructose components. **(b)** The preparation of PMWF dry electrode by solution processing method for ECG detection.

The uniform mixture of PEDOT:PSS, MXene, WPU, and fructose was poured into a model and dried thoroughly before the formation of the blend film. The resulting PMWF films are then investigated as a dry electrode for subsequent characterization and ECG measurements (**Figure 1b**).

Highly conductive MXene nanosheets are prepared by selectively etching the Al layer in $Ti_3AlC_2$ in LiF/HCl solution. After ultrasonication treatment, the exfoliated MXene monolayer colloidal dispersion in deionized water can be obtained[35]. The MXene nanosheets were characterized by X-ray diffraction (XRD) spectrum (**Figure 2a**). In the XRD pattern of raw $Ti_3AlC_2$, the characteristic peak of the MAX phase at about 39° (104) is identified[28]. After exfoliation, the absence of the characteristic (104) peak of the MAX phase indicated the formation of MXene nanosheets. Additionally, the (002) peak at ~10° of $Ti_3AlC_2$ was broadened and shifted toward the lower angle side, indicating the successful synthesis of signal layer MXene nanosheets. The obtained MXene flakes showed a remarkable (002) peak at $2\theta \approx 5.8°$, which corresponds to a lattice space of 15.2 Å[36]. In the observation of TEM and SEM images (**Figure 2b, 2c**), monolayer MXene nanosheets can be identified clearly, indicating the successful preparation of single-layer MXene[37].

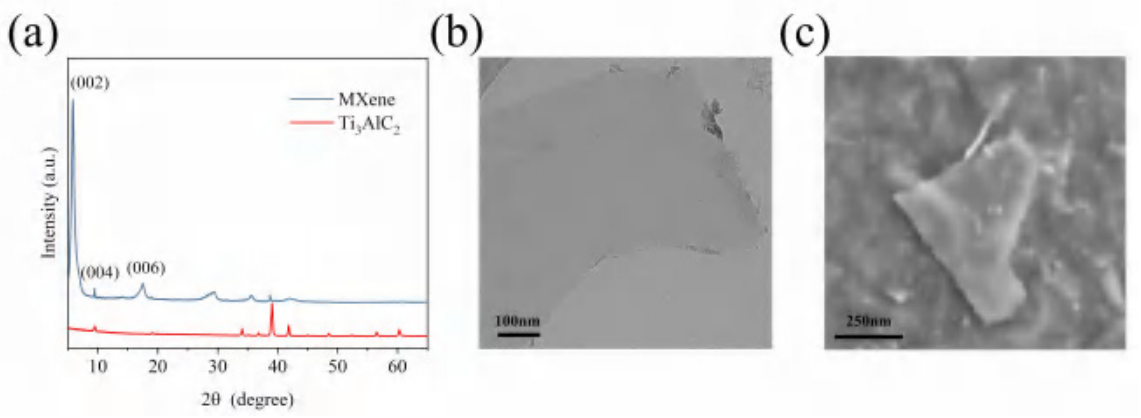


**Figure 2.** Characterization of MXene nanosheet. **(a)** XRD pattern of $Ti_3AlC_2$ and MXene nanosheets. **(b)**, **(c)** The TEM and SEM image of monolayered MXene nanosheet.

For the primary binary blend film of PEDOT:PSS and WPU (PW blend film), their stress-strain curves are shown in **Figure 3a**. With the increase of PEDOT:PSS loading, Young's modulus of PW films increased rapidly, while the elongation at break decreased accordingly. PW film with higher loading of WPU has good stretchability at the expense of conductivity. To improve the stretchability and conductivity of the PW blend film, highly conductive MXene nanosheets were added to the blend film. Additionally, fructose with multiple hydroxy groups was also added to achieve good interfacial adhesiveness to the skin. The effects of MXene nanosheets on the mechanical properties of the blend film of PEDOT:PSS, MXene, WPU and fructose (PMWF blend film) are studied with fixed loading of PEDOT:PSS (20 wt%) and fructose (5 wt%) (**Figure 3b, c**). With the addition of MXene, Young's modulus of the resulting blend film increased clearly. Upon the addition of 5 wt% MXene, Young's modulus of the PMWF blend film rapidly increased from 38.5 MPa to 101.3 MPa. Correspondingly, the elongation at break dramatically dropped from 43 % to 22 %. Therefore, MXene affects negatively the stretchability of blend films. To study the contribution of PEDOT:PSS and MXene to the conductivity of films, the weight ratio of PEDOT:PSS to MXene was set as 100:1, 20:1, 3.2:1, while the total loading of PEDOT:PSS and MXene in the PMWF blend film was constant as 21 wt%. In other words, the loading of MXene in such samples was 0.2 wt%, 1 wt%, and 5 wt%, respectively. In the measurement of sheet resistance (**Figure 3d**), it was found that an excess of MXene above 1 wt% would reduce the conductivity of the blend films, which was attributed to the aggregation of MXene nanosheets in the blend film. Given the balance between the conductivity and stretchability, 1 wt % of MXene nanosheets was added and the resultant film has a stretchability of 45% and high conductivity of 24.4 Ω/sq. The SEM image of PMWF films with 1 wt % of MXene nanosheets indicates the uniform dispersion of MXene nanosheets inside (Figure 3d inset image), coupling well with PEDOT:PSS into the conductive network[38]. Fructose plays a significant role in improving the uniform dispersion of MXene in the blend film. The resistance at different positions of PMWF films is tested (**Figure S1**). With increasing the loading of fructose, the resistances show smaller fluctuations. Also, the MXene precipitation becomes less and even has no clear aggregation (inset pictures in **Figure S1**). The above results indicate the assistance of fructose on the dispersion in PEDOT:PSS solution. The role of fructose in the mechanical property of the PMWF blend film was also investigated (**Figure 3e**). In the range of low loading below 5 wt% of fructose, the elongation at break increases gradually with increasing the loading of fructose and approaches to 53% at 5 wt% loading of fructose. However, excessive addition of fructose above 10 wt% of loading leads to lower Young's modulus and elongation at break. This phenomenon is attributed possibly to the hygroscopic properties of redundant fructose[10]. The PMWF blend film with high loading of fructose become usually fragile and even impacts the formation of a robust film. An optimal composition consisting of 20% PEDOT:PSS, 1% MXene, 5% fructose and 74% WPU is employed in this work. The prepared PMWF thin

films with 20 μm of thickness display outstanding compliance to the skin (**Figure 3f**)[6]. After peeling off, the film can preserve the epidermal wrinkle pattern, implying sufficient contact area and excellent interfacial interaction with the skin. The PMWF film has good stretchability to adapt to the movement of the wrist (**Figure S2**). On the other hand, the abundant O-H, N-H, and C=O groups provided by WPU and fructose have strong physical adsorption effects on keratin and lipids in the skin cuticle[39,40]. The standard 90-degree peel test demonstrates that PMWF films have an adhesive force above 2.2 N/m on the glass substrate and porcine skin (**Figure S3**). Benefiting from these properties, a dry electrode with low contact impedance is expected rationally.

The interfacial contact impedance between electrodes and the skin affects ECG signal quality significantly. The contact impedances of the PMWF blend films with different compositions were studied systematically. The PMWF blend film was mounted on the forearm of the subject. Two standard Ag/AgCl gel electrodes used as the counter electrode and reference electrode were attached on both sides of the PMWF film at an interval of 4 cm, respectively. The impedances between PMWF film (3 cm diameter and 20 μm thickness) and skin were measured[41].

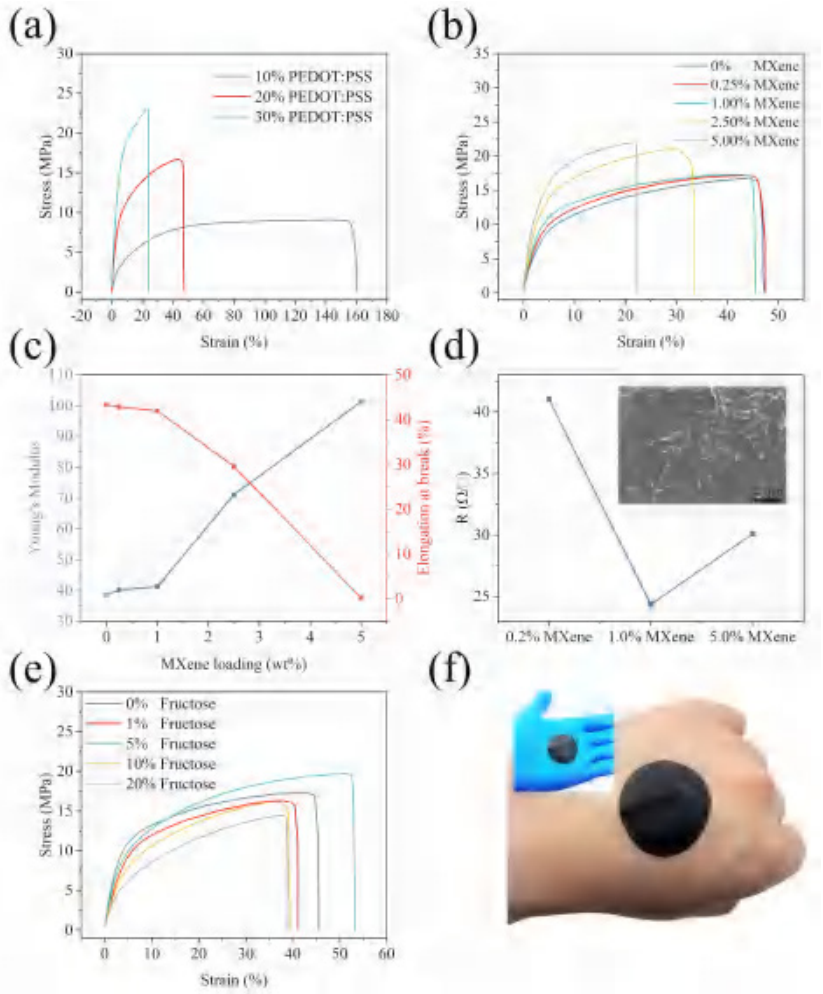


**Figure 3.** Mechanical properties characterization. **(a)** The stress-strain curves of PW blend film. **(b)** The stress-strain curves and **(c)** corresponding Young's modulus, elongation at break of PMWF blend film with different loading of MXene. The loading of PEDOT:PSS and fructose in the blend film are fixed at 20 wt% and 5 wt%, respectively. **(d)** The contribution of PEDOT:PSS and MXene to the conductivity of films. The inset is the SEM image of a PMWF blend film containing 1 wt % of MXene nanosheets. **(e)** The stress-strain curves of the PMWF blend film with different loading of fructose. The loading of PEDOT:PSS and MXene are fixed at 20 wt% and 1 wt%, respectively. **(f)** The photograph of compliant PMWF film on the skin. The epidermal wrinkle can be preserved in the PMWF film after peeling off (the inset photograph).

The impedance of PMWF blend films decreased clearly with increasing the content of PEDOT:PSS. At the loading of 20 wt% PEDOT:PSS, the impedance of PW blend film is 94.9 KΩ at 10 Hz (**Figure 4a**). When adding 1 wt% of MXene nanosheets, the impedance of the blend film decreased remarkably from 94.9 KΩ to 27.5 KΩ at 10 Hz, which is much lower than the Ag/AgCl gel electrode (256.4 KΩ). Subsequently, the impedance of PMWF blend film decrease in small amplitude when adding more MXene nanosheets (**Figure 4b**). Therefore, PMWF blends film with 1 wt% loading of MXene and 20 wt% of PEDOT:PSS is an optimal sample with low impedance without the expense of stretchability. The adhesiveness of the PMWF films arises presumably from fructose and WPU because both pristine PEDOT:PSS or MXene films are not adhesive. The surface adhesiveness of PMWF film is in favor to reduce the contact impedance.[11] With increasing the content of fructose from 1 wt% to 20 wt %, the impedance of PMWF bend film decreases from 36.17 to 11.2 KΩ at 10Hz. It is possibly attributed to the improvement of the interfacial adhesiveness with the addition of fructose.

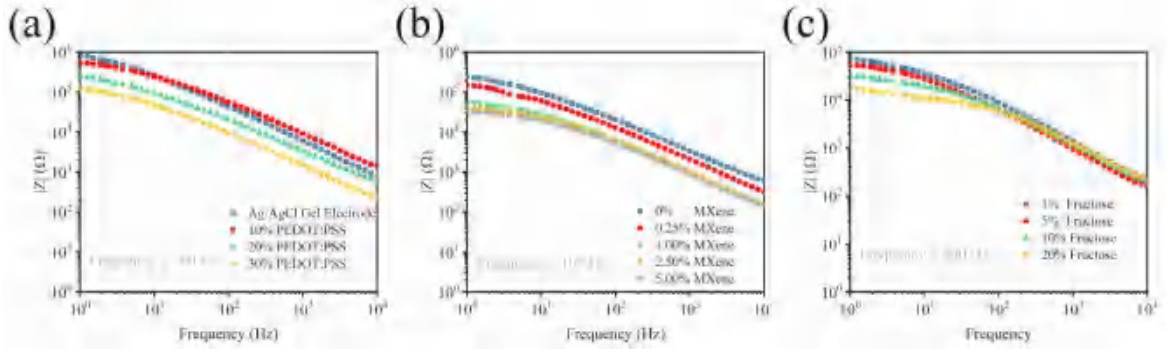


**Figure 4.** The contact impedance of PMWF blends film on the skin. **(a)** The impedance of the PMWF films with different loading of PEDOT:PSS (at constant loading of 1 wt% of MXene and 5 wt% of fructose). **(b)** The impedance of the PMWF films with different loading of MXene (at constant loading of 20 wt% of PEDOT:PSS and 5 wt% of fructose). **(c)** The impedance of the PMWF films with different loading of fructose (at constant loading of 20 wt% of PEDOT:PSS and 5 wt% of fructose).

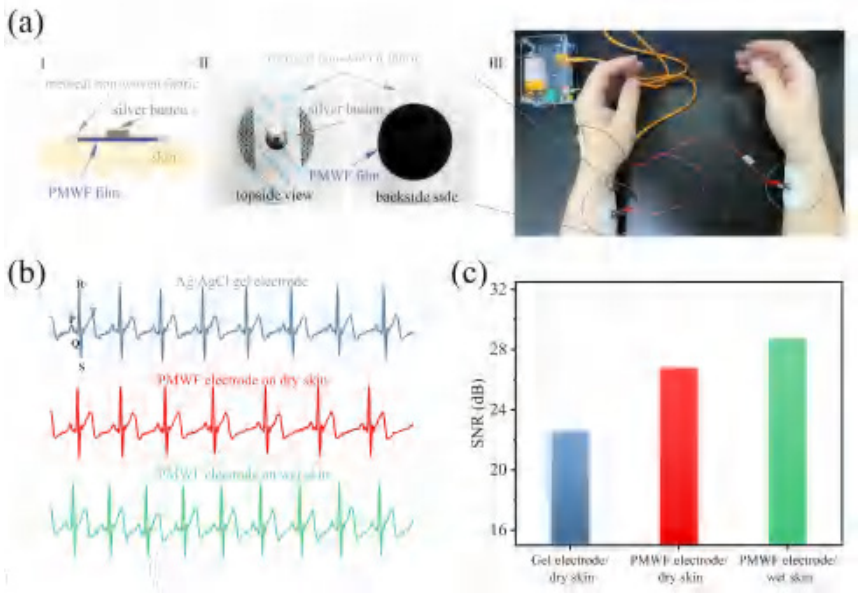


**Figure 5.** ECG signal measurement and analysis. **(a)** Preparation schematic diagram of the PMWF dry electrode **(I)** and its topside and backside view **(II)**. The fabricated PMWF dry electrode was used for ECG signal detection **(III)**. **(b)** ECG signal recorded by commercial Ag/AgCl gel electrodes and PMWF electrodes on dry and wet skin, respectively. **(c)** SNR of ECG signals measured under different conditions.

The PMWF film with low contact impedance and excellent skin compliance can be used as a wearable dry electrode to detect epidermal ECG signals. The circular PMWF films with a diameter of 3 cm were pasted on the stretchable non-woven fabric and Ag/AgCl buttons act as the electrode connector (**Figure 5a I**), assembling into a dry electrode (**Figure 5a II**). To record the ECG signals, two PMWF dry electrodes were placed symmetrically on the wrist of the left and right forearms, and the other PMWF electrode used as a reference electrode was attached to the back of the left hand (**Figure 5a III**)[10].

Due to the excellent biocompatibility, the PMWF dry electrode produces almost no irritation to the skin, so no redness of the skin is observed. The ECG signal measured using the PMWF dry electrode has a distinct PQRST waveform, which is almost identical to the waveform obtained by the standard Ag/AgCl gel electrode (**Figure 5b**). The skin was sprayed with water and formed a wet skin interface[42]. Even on the wet skin, high quality of ECG signal with distinct PQRST waveform was recorded stably by PMWF dry electrodes (**Figure 5b**), showing better detection performance on the wet skin than the gel electrode. The signal-to-noise ratio (SNR) was calculated to evaluate the signal quality (**Figure 5c**). The SNR values of PMWF dry electrodes in both dry and wet skin conditions are about 27 dB and 29 dB, respectively, which is better than those obtained by using commercial Ag/AgCl electrodes. This indicates that the electrode has a good application prospect during daily life.

## 4. Conclusion

A stretchable PMWF dry electrodes were prepared by blending PEDOT:PSS, MXene with WPU and fructose. The higher loading of PEDOT:PSS and MXene can decrease the contact impedance but also affect the stretchability of the PMWF film. The addition of fructose can improve the surface adhesiveness of PMWF and improve its compliance with the skin. Thus, the PMWF films with high loading of fructose have lower impedance. Given the balance between low impedance and good stretchability, an optimal composition of 20 wt% PEDOT:PSS 1 wt% MXene, 5 wt% fructose and 74 wt % of WPU was determined to achieve a dry electrode. The obtained PMWF dry electrode has outstanding skin compliance and low contact impedance with skin. They can be used to acquire high-quality ECG signals under various skin conditions including dry and wet scenarios. The SNR of PMWF dry electrode is over 25 dB, which is superior to the commercial Ag/AgCl electrodes and other dry electrodes in the literature. Therefore, these PMWF dry electrodes have great promise in wearable ECG measurement in daily scenarios.

## Acknowledgement

This research work was financially supported by the fundamental research funds for the central universities (No. 226-2022-00083) and the one-hundred-person project of Zhejiang University.

## Conflict of Interest

The authors declare no conflict of interest.

## Reference

[1] Luo Z, Peng B, Zeng J, *et al*. Sub-thermionic, ultra-high-gain organic transistors and circuits. *Nature Communications*, 2021; *12*(1):1928. https://doi.org/10.1038/s41467-021-22192-2.

[2] Park T, Jeong J, Kim Y J, *et al*. Weak Molecular Interactions in Organic Composite Dry Film Lead to Degradable, Robust Wireless Electrophysiological Signal Sensing. *Advanced Materials Interfaces*, 2022; *9*(24):2200594. https://doi.org/10.1002/admi.202200594.

[3] Wang L-F, Liu J-Q, Dong Y, *et al*. Polydimethylsiloxane film for biomimetic dry adhesive integrated with capacitive biopotentials sensing. *Sensors and Actuators B: Chemical*, 2014; *205*:168-175. https://doi.org/10.1016/j.snb.2014.08.069.

[4] Niu X, Gao X, Wang T, *et al*. Ordered Nanopillar Arrays of Low Dynamic Noise Dry Bioelectrodes for Electrocardiogram Surface Monitoring. *ACS Applied Materials & Interfaces*, 2022; *14*(29):33861-33870. https://doi.org/10.1021/acsami.2c08318.

[5] Miyamoto A, Lee S, Cooray N F, *et al*. Inflammation-free, gas-permeable, lightweight, stretchable on-skin electronics with nanomeshes. *Nature Nanotechnology*, 2017; *12*(9):907-913. https://doi.org/10.1038/nnano.2017.125.

[6] Wang Y, Lee S, Wang H, *et al*. Robust, self-adhesive, reinforced polymeric nanofilms enabling gas-permeable dry electrodes for long-term application. *Proceedings of the National Academy of Sciences*, 2021; *118*(38):e2111904118. https://doi.org/10.1073/pnas.211190411.

[7] Napier B S, Matzeu G, Presti M L, *et al*. Dry Spun, Bulk-Functionalized rGO Fibers for Textile Integrated Potentiometric Sensors. *Advanced Materials Technologies*, 2022; *7*(6):2101508. https://doi.org/10.1002/admt.202101508.

[8] Gao L, Wang X, Dai W, *et al*. Laser Direct Writing Assisted Fabrication of Skin Compatible Metal Electrodes. *Advanced Materials Technologies*, 2020; *5*(5):2000012. https://doi.org/10.1002/admt.202000012.

[9] Nigusse A B, Mengistie D A, Malengier B, *et al*. Wearable Smart Textiles for Long-Term Electrocardiography Monitoring-A Review. *Sensors (Basel)*, 2021; *21*(12). https://doi.org/10.3390/s21124174.

[10] Gao D, Parida K and Lee P S. Emerging Soft Conductors for Bioelectronic Interfaces. *Advanced Functional Materials*, 2020; *30*(29):1907184. https://doi.org/10.1002/adfm.201907184.

[11] Zhang L, Kumar K S, He H, *et al*. Fully organic compliant dry electrodes self-adhesive to skin for long-term motion-robust epidermal biopotential monitoring. *Nature Communications*, 2020; *11*(1):4683. https://doi.org/10.1038/s41467-020-18503-8.

[12] Cheng Y, Zhou Y, Wang R, *et al*. An Elastic and Damage-Tolerant Dry Epidermal Patch with Robust Skin Adhesion for Bioelectronic Interfacing. *ACS Nano*, 2022; *16*(11):18608-18620. https://doi.org/10.1021/acsnano.2c07097.

[13] Chiu C-W, Huang C-Y, Li J-W, *et al*. Flexible Hybrid Electronics Nanofiber Electrodes with Excellent Stretchability and Highly Stable Electrical Conductivity for Smart Clothing. *ACS Applied Materials & Interfaces*, 2022; *14*(37):42441-42453. https://doi.org/10.1021/acsami.2c11724.

[14] Yao S, Zhou W, Hinson R, *et al*. Ultrasoft Porous 3D Conductive Dry Electrodes for Electrophysiological Sensing and Myoelectric Control. *Advanced Materials Technologies*, 2022; *7*(10):2101637. https://doi.org/10.1002/admt.202101637.

[15] Park C, Kim M S, Kim H H, *et al*. Stretchable conductive nanocomposites and their applications in wearable devices. *Applied Physics Reviews*, 2022; *9*(2). https://doi.org/10.1063/5.0093261.

[16] Lee S M, Byeon H J, Lee J H, *et al*. Self-adhesive epidermal carbon nanotube electronics for tether-free long-term continuous recording of biosignals. *Scientific Reports*, 2015; *4*(1):6074. https://doi.org/10.1038/srep06074.

[17] Solorio-Rodriguez S A, Williams A, Poulsen S S, *et al*. Single-Walled vs. Multi-Walled Carbon Nanotubes: Influence of Physico-Chemical Properties on Toxicogenomics Responses in Mouse Lungs. *Nanomaterials (Basel)*, 2023; *13*(6). https://doi.org/10.3390/nano13061059.

[18] Zhang Y, Xue Q, Yin X, *et al*. Reproductive Toxicity Evaluation of Graphene-Based Tumor Cell Nucleus-Targeting Fluorescent Nanoprobes on Reproduction and Offspring Health. *Mol Pharm*, 2023. https://doi.org/10.1021/acs.molpharmaceut.2c00934.

[19] Choi S, Raja I S, Selvaraj A R, *et al*. Activated carbon nanofiber nanoparticles incorporated electrospun polycaprolactone scaffolds to promote fibroblast behaviors for application to skin tissue engineering. *Advanced Composites and Hybrid Materials*, 2022; *6*(1). https://doi.org/10.1007/s42114-022-00608-x.

[20] Lo L-W, Zhao J, Aono K, *et al*. Stretchable Sponge Electrodes for Long-Term and Motion-Artifact-Tolerant Recording of High-Quality Electrophysiologic Signals. *ACS Nano*, 2022; *16*(8):11792-11801. https://doi.org/10.1021/acsnano.2c04962.

[21] Kayser L V and Lipomi D J. Stretchable Conductive Polymers and Composites Based on PEDOT and PEDOT:PSS. *Adv Mater*, 2019; *31*(10):e1806133. https://doi.org/10.1002/adma.201806133.

[22] Li T, Liang B, Ye Z, *et al*. An integrated and conductive hydrogel-paper patch for simultaneous sensing of Chemical–Electrophysiological signals. *Biosensors and Bioelectronics*, 2022; *198*:113855. https://doi.org/10.1016/j.bios.2021.113855.

[23] Roberts T, De Graaf J B, Nicol C, *et al*. Flexible Inkjet-Printed Multielectrode Arrays for Neuromuscular Cartography. *Advanced Healthcare Materials*, 2016; *5*(12):1462-1470. https://doi.org/10.1002/adhm.201600108.

[24] Kim Y, Yoo S and Kim J H. Water-Based Highly Stretchable PEDOT:PSS/Nonionic WPU Transparent Electrode. *Polymers (Basel)*, 2022; *14*(5). https://doi.org/10.3390/polym14050949.

[25] He H and Ouyang J. Enhancements in the Mechanical Stretchability and Thermoelectric Properties of PEDOT:PSS for Flexible Electronics Applications. *Accounts of Materials Research*, 2020; *1*(2):146-157. https://doi.org/10.1021/accountsmr.0c00021.

[26] Wang Y, Zhu C, Pfattner R, *et al*. A highly stretchable, transparent, and conductive polymer. *Science Advances*, 2017; *3*(3):e1602076. https://doi.org/10.1126/sciadv.1602076.

[27] Zhao Y, Zhang S, Yu T, *et al*. Ultra-conformal skin electrodes with synergistically enhanced conductivity for long-time and low-motion artifact epidermal electrophysiology. *Nature Communications*, 2021; *12*(1):4880. https://doi.org/10.1038/s41467-021-25152-y.

[28] Han M, Shuck C E, Rakhmanov R, *et al*. Beyond Ti(3)C(2)T(x): MXenes for Electromagnetic Interference Shielding. *ACS Nano*, 2020; *14*(4):5008-5016. https://doi.org/10.1021/acsnano.0c01312.

[29] Zuo X, Fan T, Qu L, *et al*. Smart multi-responsive aramid aerogel fiber enabled self-powered fabrics. *Nano Energy*, 2022; *101*:107559. https://doi.org/10.1016/j.nanoen.2022.107559.

[30] Miao J and Fan T. Flexible and stretchable transparent conductive graphene-based electrodes for emerging wearable electronics. *Carbon*, 2023; *202*:495-527. https://doi.org/10.1016/j.carbon.2022.11.018.

[31] Zhang W, Miao J, Tian M, *et al*. Hierarchically interlocked helical conductive yarn enables ultra-stretchable electronics and smart fabrics. *Chemical Engineering Journal*, 2023; 462:142279. https://doi.org/10.1016/j.cej.2023.142279.

[32] Xu P, Lu C, Wang D, *et al*. Combination of ultrathin micro-patterned MXene and PEDOT: Poly(styrenesulfonate) enables organic electrochemical transistor for amperometric determination of survivin protein in children osteosarcoma. *Microchimica Acta*, 2021; *188*(9):301. https://doi.org/10.1007/s00604-021-04947-2.

[33] Li X, An Z, Lu Y, *et al*. Room Temperature VOCs Sensing with Termination-Modified Ti3C2Tx MXene for Wearable Exhaled Breath Monitoring. *Advanced Materials Technologies*, 2022; *7*(3):2100872. https://doi.org/10.1002/admt.202100872.

[34] Li P, Du D, Guo L, *et al*. Stretchable and conductive polymer films for high-performance electromagnetic interference shielding. *Journal of Materials Chemistry C*, 2016; *4*(27):6525-6532. https://doi.org/10.1039/C6TC01619G.

[35] Ma J, Cheng Y, Wang L, *et al*. Free-standing $Ti_3C_2T_x$ MXene film as binder-free electrode in capacitive deionization with an ultrahigh desalination capacity. *Chemical Engineering Journal*, 2020; *384*: 123329.

[36] Ding H, Zeng Z, Wang Z, *et al*. Deep Learning-Enabled MXene/PEDOT:PSS Acoustic Sensor for Speech Recognition and Skin-Vibration Detection. *Advanced Intelligent Systems*, 2022; *4*(10):2200140. https://doi.org/10.1016/j.cej.2019.123329.

[37] Wang H, Zhang J, Wu Y, *et al*. Achieving high-rate capacitance of multi-layer titanium carbide (MXene) by liquid-phase exfoliation through Li-intercalation. *Electrochemistry Communications*, 2017; *81*:48-51. https://doi.org/10.1016/j.elecom.2017.05.009.

[38] Zeng R, Wang W, Chen M, *et al*. CRISPR-Cas12a-driven MXene-PEDOT:PSS piezoresistive wireless biosensor. *Nano Energy*, 2021; *82*:105711. https://doi.org/10.1016/j.nanoen.2020.105711.

[39] Guo R, Sun X, Yuan B, *et al*. Magnetic Liquid Metal (Fe-EGaIn) Based Multifunctional Electronics for Remote Self-Healing Materials, Degradable Electronics, and Thermal Transfer Printing. *Advanced Science*, 2019; *6*(20):1901478. https://doi.org/10.1002/advs.201901478.

[40] Sun Y, Wang S, Du X, *et al*. Skin-conformal MXene-doped wearable sensors with self-adhesive, dual-mode sensing, and high sensitivity for human motions and wireless monitoring. *Journal of Materials Chemistry B*, 2021;

*9*(41):8667-8675. https://doi.org/10.1039/D1TB01769A.

[41] Ershad F, Thukral A, Yue J, *et al*. Ultra-conformal drawn-on-skin electronics for multifunctional motion artifact-free sensing and point-of-care treatment. *Nature Communications*, 2020; *11*(1):3823. https://doi.org/10.1038/s41467-020-17619-1.

[42] Robinson S and Robinson A H. Chemical Composition of Sweat. *Physiological Reviews*, 1954; *34*(2):202-220. https://doi.org/10.1152/physrev.1954.34.2.202.